STIFFNESS MATRIX ANALYSIS OF SIX-REVOLUTE SERIAL MANIPULATOR

Józef KNAPCZYK* , **Mateusz RYSKA***

*Cracow University of Technology, Al. Jana Pawła II 37 b, 31-864 Kraków, Poland

j_kn@mech.edu.pl, mateusz.ryska@o2.pl

Abstract: This paper presents a simple procedure that can be used to determine the stiffness matrix of 6R serial manipulator in selected points of the work space with joint stiffness coefficients taking into account. Elastokinematical model for the robot manipulator FANUC S-420F was considered as spatial and serial kinematical chain composed of six rigid links, connected by ideal revolute joint (without clearances and deformable elements), with torsion elasticity of the joint drive system (relative torsion deformations are proportional to acted torques) taking into account. Assumed model is used for displacement analysis of the end-effector for a given applied force in quasi-static condition. The analysis results are presented as Cartesian stiffness matrix of studied manipulator.

Key words: Serial Manipulator, Jacobian Matrix, Cartesian Stiffness Matrix

1. INTRODUCTION

Serial robots are mainly used in industry for the tasks required good repeatability but not necessarily high accuracy of the end-effector pose in workspace (position and orientation according to ISO9283). For example, these robots are used for pick-and-place, painting and welding operations. Nevertheless, many serial robots are now used for machining operations that require high precision and stiffness.

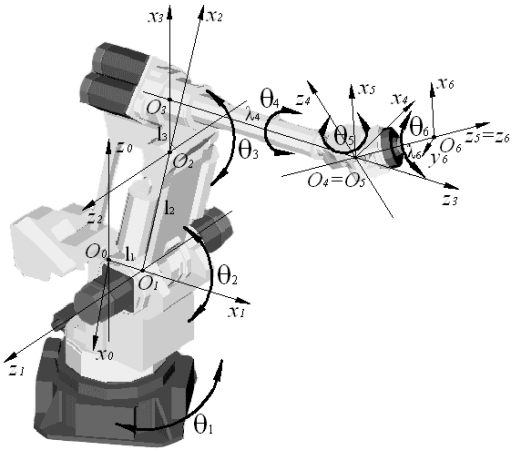

Fig. 1. Industrial Robot FANUC S-420F (Kim and Treit, 1995)

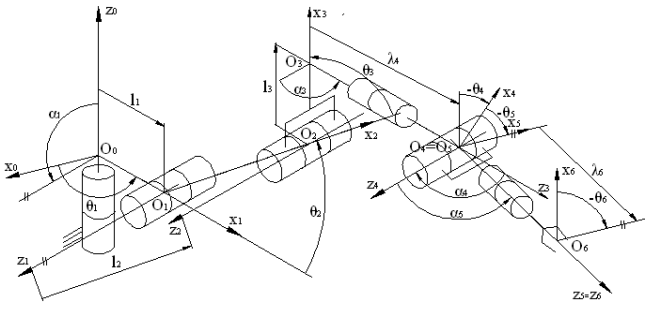

Fig. 2. Kinematical model of manipulator 6R FANUC S-420F

Elastokinematical models of serial manipulators are used for stiffness analysis and presented in: Dumas et al. (2011), Góra and Trela (2011a, b), Kim and Treit (1995) and Morecki et al. (1995); however, the identification of stiffness parameters has yet to be determined. Two methods were used to obtain the Cartesian stiffness matrix of serial manipulator. The first method consists of clamping all of the joints except one to measure its elastic deflection under applied load. The joint stiffness matrix of manipulator is obtained by repeating the procedure for each revolute joint. Therefore, only six experiments are required with this method to evaluate stiffness matrix of the 6R manipulator throughout its workspace. The second method measures the displacements of the end-effector due to certain applied loads and evaluates the stiffness matrix throughout its workspace with some interpolations. This method gives better results than the first when many tests are performed under different manipulator configurations.

This paper presents the Cartesian stiffness matrix analysis of the 6R robot FANUC S-420F (see Figs. 1 i 2).

2. STIFFNESS MATRIX FORMULATION

Kinematical model of 6R robot manipulator (FANUC S-420F) is considered as serial kinematical chain with six revolute joints (Fig.2). Denavit-Hartenberg (D-H) parameters are given in Tab. 1.

The (6×6) Jacobian matrix of the manipulator is:

$$\mathbf{J} = \left[\frac{\partial p_x}{\partial \theta_i} \;\; \frac{\partial p_y}{\partial \theta_i} \;\; \frac{\partial p_{xz}}{\partial \theta_i} \;\; \frac{\partial \varphi_x}{\partial \theta_i} \;\; \frac{\partial \varphi_y}{\partial \theta_i} \;\; \frac{\partial \varphi_z}{\partial \theta_i}\right]^T \tag{1}$$

where: p_x, p_y, p_z – point coordinates of the end-effector; φ_x, φ_y, φ_z – angular coordinates of the end-effector with respect to the base frame axes, θ_i – angular coordinate of the revolute joint i (i = 1, 2, ...6).

The links of the robot are assumed as rigid bodies, and the joint stiffness (with control loop stiffness and actuators mechanical stiffness taking into account) is represented with linear torsion spring. In the case of small elastic deformation the following relation can be written (Dumas et al., 2011; Kim and Treit, 1995; Tsai, 1999):

$$m_i = k_i \Delta\theta_i \tag{2}$$

where: m_i – torque applied on the joint i, $\Delta\theta_i$ – torsion deformation, k_i – i -th joint stiffness value .

Assuming that frictional forces at the joints are negligible and neglecting the gravitational effect we can apply the principle of virtual work to derive a transformation between the joint torques and end-effector forces:

$$\mathbf{m} = \mathbf{J}^T\mathbf{f} \tag{3}$$

where: $\mathbf{m} = [m_1 \dots m_6]^T$, $\mathbf{f} = [F_x\ F_y\ F_z\ M_x\ M_y\ M_z]^T$,
$\mathbf{f}$ – vector of the end-effector output force and moment (the components are described with respect to the base frame); $\Delta\mathbf{d}$ – displacement of the end-effector (in Cartesian coordinates) as proportional to the quasi-static output load:

$$\Delta\mathbf{d} = \mathbf{C}\mathbf{f} = \mathbf{K}^{-1}\mathbf{f} \tag{4}$$

where: $\Delta\mathbf{d} = [\Delta p_x\ \Delta p_y\ \Delta\ p_z\ \Delta\varphi_x\ \Delta\varphi_y\ \Delta\ \varphi_z]^T$

$$\mathbf{K} = \mathbf{J}^{-T}(\mathbf{K}_\theta - \mathbf{K}_C)\mathbf{J}^{-1} \tag{5}$$

$$\begin{aligned} &\mathbf{K}_\theta = diag[k_1 k_2 \dots\ k_6] \\ &\mathbf{K}_C = \left[\frac{\partial \mathbf{J}^T}{\partial \theta_i}\right]\mathbf{m} \quad (i = 1, 2, \dots 6) \end{aligned} \tag{6}$$

$\mathbf{C}\,(6\mathrm{x}6)$ – compliance matrix, $\mathbf{K}\,(6\mathrm{x}6)$ – stiffness matrix of manipulator, $\mathbf{K}_\theta$ – diagonal joint stiffness matrix, $\mathbf{J}$ – kinematical Jacobian matrix, $\mathbf{K}_C$ – complementary stiffness matrix. According to (5) stiffness matrix of manipulator depends on both constant matrix $\mathbf{K}_\theta$ and variable matrix $\mathbf{K}_C$, depended on position. It make sense that joint stiffness identification is easier when $\mathbf{K}_C$ is negligible with respect to $\mathbf{K}_\theta$. From equations (4) and (5) it can be derived:

$$\Delta\mathbf{d} \cong \mathbf{J}\mathbf{K}_\theta^{-1}\mathbf{J}^T\mathbf{f} \tag{7}$$

Let the joint compliances be the components of the six-dimensional vector:

$$\boldsymbol{\kappa} = [\kappa_i]^T = [1/k_i]^T \quad (i = 1, 2, \dots 6) \tag{8}$$

The 6-dimensional vector (7) describing small displacement of the end-effector can be expressed as:

$$\Delta\mathbf{d} = \mathbf{F}\boldsymbol{\kappa} \tag{9}$$

where:

$$\mathbf{F} = \begin{bmatrix} J_{11}\sum_{i=1}^{6} J_{i1}f_i & \dots & J_{16}\sum_{i=1}^{6} J_{i6}f_i \\ \dots & \dots & \dots \\ J_{61}\sum_{i=1}^{6} J_{i1}f_i & \dots & J_{66}\sum_{i=1}^{6} J_{i6}f_i \end{bmatrix} \tag{10}$$

Therefore, $\mathbf{f}$ – vector of load , $\Delta\mathbf{d}$ – vector of displacement and matrix $\mathbf{F}$ are associated with each test in determined position and load case. When only one test is considered, then matrix $\mathbf{F}$ is $(6\mathrm{x}6)$. If it is nonsingular, then equation (9) has a unique solution (Dumas et al., 2011):

$$\boldsymbol{\kappa} = \mathbf{F}^{-1}\Delta\mathbf{d} \tag{11}$$

When several tests are considered, the equation system (9) becomes over-determined. Assuming that *n* tests are taken into account, matrix $\mathbf{F}$ becomes $(6n\mathrm{x}6)$, no longer square matrix, and the joint compliance vector $\boldsymbol{\kappa}$ cannot be calculated using (11), because the number of equations is higher than the number of unknowns. In this case it is possible to find a vector $\boldsymbol{\kappa}$ that minimizes the Euclidean norm of the approximation error of the system. From equation system (9) it is apparent that the higher the number of tests gives the higher the degree of constraint of the equation system, and the more accurate solution, i.e., the more accurate evaluation of the joint stiffness values. Obviously, the higher number of tests is connected with the more expensive identification procedure. Therefore, it is suggested to find compromise between identification accuracy and cost, for example five tests are a good compromise.

It is possible to identify the stiffness values of the first three joints of a six-revolute manipulator by measuring only the translational displacements of its end-effector loaded by force.

2.1. Numerical example

Problem is to determine the stiffness matrix of manipulator Fanuc S-420F, with only torsion flexibility in the first three joints taking into account. For a given vertical force applied on the end-effector its linear displacements are measured. The robot with the end-effector loaded be gravity force is shown in Fig. 3. The measurement results are presented as compliance characteristics on Fig. 4.

The D-H parameters of the considered manipulator are given in Tab. 1. The first three elements of the compliance matrix, that influenced on the linear displacement of the end-effector, are presented in Apendix A.

Tab. 1. D-H parameters of manipulator Fanuc S-420F

l	α_i[°]	l_i[mm]	λ_i[mm]	θ_i[°]
1	90	270	0	±150
2	0	900	0	±57,5
3	90	270	0	±72,5
4	-90	0	1300	±360
5	90	0	0	±125
6	0	0	260	±360

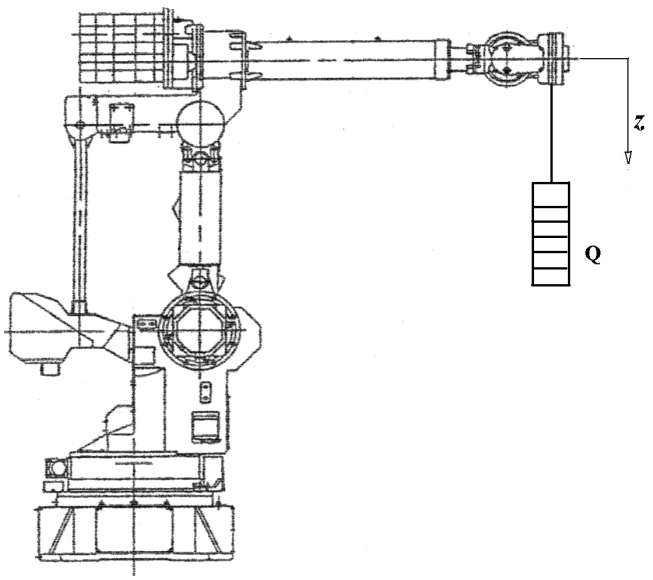

Fig. 3. Robot manipulator Fanuc S-420F with the end-effector loaded by vertical force Q

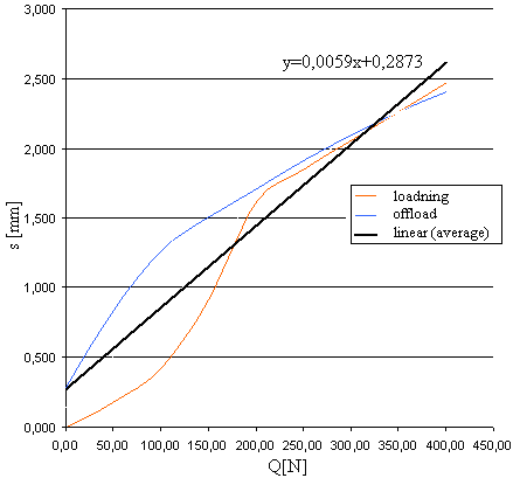

Fig. 4. Compliance characteristics (s – vertical displacement of the end-effector of robot Fanuc S-420F with respect to Q – vertical force), determined on the basis of stand measurement results

A comparison between joint stiffness data as given in Kim and Treit (2011) for robot PUMA 560: k_1=66.230; k_2=66.50; k_3=11.610; k_4=0.202; k_5=0.101; k_6=0.144 [kNm/rad]; given in Dumas et al. (2011) for robot Kuka KR240-2: k_1=1.410; k_2=0.401; k_3=0.935; k_4=0.360; k_5=0.370; k_6=0.380 [kNm/rad].

Measurements of Cartesian coordinates of the end-effector loaded by vertical force are as follows:

$$p_x = 279.85;\ p_y = 2751.95;\ p_z = 145.14\ [\mathrm{mm}];$$

$$\varphi_x = 89.34;\ \varphi_y = 46.57;\ \varphi_z = 0.73\ [^\circ].$$

By solving the inverse kinematical problem the respective joint coordinates are obtained:

$$\theta_i = -84.91^\circ;\ 65.00^\circ;\ -12.31^\circ;\ 0.00^\circ;\ 9.64^\circ;\ 0.00^\circ$$

Assuming that joint stiffness coefficients of the considered manipulator Fanuc S-420F are the same as given values for manipulator PUMA 560 and using formulae (A3) for the $(3\mathrm{x}3)$ element of the stiffness and compliance matrix were calculated $c_{33} = 0.00183\ [\mathrm{mm/N}];\ k_{33} = 546.6\ [\mathrm{mm/N}]$. Respective values of this element determined on the basis of measurements made for manipulator Fanuc S-420F are: $c_{33} = 0.0059\ [\mathrm{mm/N}];\ k_{33} = 169.5\ [\mathrm{mm/N}]$.

Suggestions for explaining this difference include variations between assumed and real values of joint stiffness coefficients. It can be concluded that stiffness coefficients of the first three joints of manipulator Fanuc S-420F are about three times greater than the respective given for manipulator PUMA 560.

3. CONCLUSION

The subject of this paper was to describe a method for stiffness analysis of serial manipulator. Elastokinematical model of the considered manipulator was assumed with the links as rigid bodies, and with the linear torsion springs in revolute joints (with control loop stiffness and actuators mechanical stiffness taking into account). Numerical example for the stiffness matrix of manipulator Fanuc S-420F is given. Cartesian stiffness matrix obtained by using presented method can be applied for planning the Cartesian trajectory of the end-effector with its load taken into account, for example tool path planning considering robot performance indices.

REFERENCES

1. **Dumas C. et al.** (2011), Joint stiffness identification of six-revolute industrial serial robots. *Robotics and Computer-Integrated Manufacturing* 27, 881-888.
2. **Góra M., Trela R.** (2011a), Determination of stiffness characteristics of serial type manipulator by using wire sensors. *Technical Transactions,Czasopismo Techniczne,* Wyd. PK, Kraków, 1M/2011, 41-48.
3. **Góra M., Trela R.** (2011b), Experimental determination of stiffness matrix elements of serial type manipulator, *Pomiary Automatyka Robotyka*, 2/2011, 687-696.
4. **Kim H.Y., Treit D.A.** (1995), Configuration dependent stiffness of the PUMA 560 manipulator: Analytical and experimental results. *Mechanism and Machine Theory,* Vol.30, No 8, 1269-1277.
5. **Morecki A., Knapczyk J., Kędzior K.** (2002), *Theory of mechanisms and manipulators*, WNT Warszawa.
6. **Tsai L.W.,** (1999), *Robot Analysis. The Mechanics of Serial and Parallel Manipulators*, A Wiley & Sons, Inc. New York.

APPENDIX: DIAGONAL ELEMENTS OF COMPLIANCE MATRIX C (4) FOR MANIPULATOR FANUC S-420F (D-H parameters are given in Tab.1)

$$\begin{aligned}
c_{11} &= \frac{1}{\kappa_1}\left[\left(-s_1\left(l_1 + l_2c_2 + l_3c_{23} + s_{23}\lambda_4\right) - \lambda_6\left(\left(s_1c_{23}c_4 - c_1s_4\right)s_5 + s_1s_{23}c_5\right)\right)^2\right] + \\
&+ \frac{1}{\kappa_2}\left[c_1^2\left(l_2s_2 + l_3c_{23} - c_{23}\lambda_4 + \left(s_{23}c_4s_5 - c_{23}c_5\right)\lambda_6\right)^2\right] + \\
&+ \frac{1}{\kappa_3}\left[c_1^2\left(l_3s_{23} - c_{23}\lambda_4 + \left(s_{23}c_4s_5 - c_{23}c_5\right)\lambda_6\right)^2\right] + \\
&+ \frac{1}{\kappa_4}\left[\lambda_6^2\left(\begin{array}{l} s_1s_{23}\left(-c_{23}\lambda_4 + s_{23}c_4s_5 - c_{23}c_5\right) + \\ + c_{23}\left(s_1s_{23}\lambda_4 + \left(s_1c_{23}c_4 - c_1s_4\right)s_5 + s_1s_{23}c_5\right)\end{array}\right)^2\right] + \\
&+ \frac{1}{\kappa_5}\left[\lambda_6^2\left(\left(-s_1c_{23}s_4 - c_1c_4\right)\left(s_{23}c_4s_5 - c_{23}c_5\right) + s_{23}s_4\left(\left(s_1c_{23}c_4 - c_1s_4\right)s_5 + s_1s_{23}c_5\right)\right)^2\right]
\end{aligned} \qquad \text{(A.1)}$$

$$
\begin{aligned}
c_{22} &= \frac{1}{\kappa_1}\left(\left[c_1\left(l_1 + l_2c_2 + l_3c_{23} + s_{23}\lambda_4\right) + \lambda_6\left(\left(c_1c_{23}c_4 + c_1s_4\right)s_5 + s_1s_{23}c_5\right)^2\right]\right) + \\
&+ \frac{1}{\kappa_2}\left[s_1^2\left(l_2s_2 + l_3s_{23} - c_{23}\lambda_4 + \left(s_{23}c_4s_5 - c_{23}c_5\right)\lambda_6\right)^2\right] + \\
&+ \frac{1}{\kappa_3}\left[s_1^2\left(l_3s_{23} - c_{23}\lambda_4 + \left(s_{23}c_4s_5 - c_{23}c_5\right)\lambda_6\right)^2\right] + \\
&+ \frac{1}{\kappa_4}\left[\lambda_6^2\left(\begin{array}{l} -c_{23}\left(c_1s_{23}\lambda_4 + \left(c_1c_{23}c_4 + s_1s_4\right)s_5 + c_1s_{23}c_5\right) - \\ -c_1s_{23}\left(-c_{23}\lambda_4 + s_{23}c_4s_5 - c_{23}c_5\right)\end{array}\right)^2\right] + \\
&+ \frac{1}{\kappa_5}\left[\lambda_6^2\left(-s_{23}s_4\left(\left(c_1c_{23}c_4 + s_1s_4\right)s_5 + c_1s_{23}c_5\right) + \left(c_1c_{23}s_4 - s_1c_4\right)\left(s_{23}c_4s_5 - c_{23}c_5\right)\right)^2\right]
\end{aligned}
\tag{A.2}
$$

$$
\begin{aligned}
c_{33} &= \frac{1}{\kappa_2}\left[\left(s_1\left(s_1\left(l_1 + l_2c_2 + l_3c_{23} + s_{23}\lambda_4\right) + \lambda_6\left(\left(s_1c_{23}c_4 - c_1s_4\right)s_5 + s_1s_{23}c_5\right)\right) + \right.\right. \\
&\left.\left. + c_1\left(c_1\left(l_2s_2 + l_3c_{23} + s_{23}\lambda_4\right) + \left(\left(c_1c_{23}c_4 + s_1s_4\right)s_5 + c_1s_{23}c_5\right)\lambda_6\right)\right)^2\right] + \\
&\left(+\left(s_{23}c_4s_5 - c_{23}c_5\right)\lambda_6\right) \\
&+ \frac{1}{\kappa_3}\left[\left(s_1\left(s_1\left(l_3c_{23} + s_{23}\lambda_4\right) + \lambda_6\left(\left(s_1c_{23}c_4 - c_1s_4\right)s_5 + s_1s_{23}c_5\right)\right) + \right.\right. \\
&\left.\left. + c_1\left(c_1\left(l_3c_{23} + s_{23}\lambda_4\right) + \left(\left(c_1c_{23}c_4 - c_1s_4\right)s_5 + c_1s_{23}c_5\right)\lambda_6\right)\right)^2\right] + \\
&+ \frac{1}{\kappa_4}\left[\left(c_1s_{23}\left(s_1s_{23}\lambda_4 + \lambda_6\left(\left(s_1c_{23}c_4 - c_1s_4\right)s_5 + s_1s_{23}c_5\right) - \right.\right.\right. \\
&\left.\left.\left. - s_1s_{23}\left(c_1s_{23}\lambda_4 + \left(\left(c_1c_{23}c_4 + s_1s_4\right)s_5 + s_1s_{23}c_5\right)\lambda_6\right)\right)^2\right] + \\
&+ \frac{1}{\kappa_5}\left[\lambda_6^2\left(\left(-c_1c_{23}s_4 + s_1c_4\right)\left(\left(s_1c_{23}c_4 - c_1s_4\right)s_5 + s_1s_{23}c_5\right) + \right.\right. \\
&\left.\left. + \left(s_1c_{23}s_4 + c_1c_4\right)\left(\left(c_1c_{23}c_4 + s_1s_4\right)s_5 + c_1s_{23}c_5\right)\right)^2\right]
\end{aligned}
\tag{A.3}
$$

where $c_i = \cos\theta_i, s_i = \sin\theta_i,\ c_{ij} = \cos(\theta_i + \theta_j),\ s_{ij} = \sin(\theta_i + \theta_j)$